Translational Oncology 13 (2020) 100751

Contents lists available at ScienceDirect

Translational Oncology

journal homepage: www.elsevier.com/locate/tranon

The JNK inhibitor AS602801 Synergizes with Enzalutamide to Kill Prostate Cancer Cells *In Vitro* and *In Vivo* and Inhibit Androgen Receptor Expression ☆

Zhenghong Li [a,b], Carrie Sun [c], Sijia Tao [d], Adeboye O. Osunkoya [a,c,e,f], Rebecca S. Arnold [c], John A. Petros [a,c,e,f], Xiongbing Zu [b], Carlos S. Moreno [a,e,*]

[a] Department of Pathology and Laboratory Medicine, Emory University, Atlanta, GA 30322, USA
[b] Department of Urology, Xiangya Hospital, Central South University, Changsha, Hunan Province, 410008, China
[c] Department of Urology, Emory University, Atlanta, GA 30322, USA
[d] Department of Pediatrics, Emory University, Atlanta, GA 30322, USA
[e] Winship Cancer Institute, Emory University, Atlanta, GA 30322
[f] Atlanta VA Medical Center, Decatur, GA 30033

ARTICLE INFO

Article history:
Received 3 February 2020
Accepted 26 February 2020
Available online xxxx

ABSTRACT

In our previous study, we observed that androgen deprivation therapy (ADT) may induce a compensatory increase in MAPK or JNK signaling. Here, we tested the effects of the MEK inhibitors PD0325901 and GSK1120212, ERK1/2 inhibitor GDC-0994, and the JNK inhibitor AS602801 alone and in combination with the AR inhibitor enzalutamide (ENZ) in androgen-sensitive LNCaP cells and androgen-resistant C4-2 and 22Rv1 cells. Enzalutamide combined with AS602801 synergistically killed LNCaP, C4-2, and 22Rv1 cells, and decreased migration and invasion of LNCaP and C4-2 cells. We studied the combination of enzalutamide with AS602801 *in vivo* using luciferase labeled LNCaP xenografts, and observed that combination of ENZ with AS602801 significantly suppressed tumor growth compared with either drug alone. Importantly, combination therapy resulted in dramatic loss of AR mRNA and protein. Surprisingly, mechanistic studies and Nanostring data suggest that AS602801 likely activates JNK signaling to induce apoptosis. Since AS602801 had sufficient safety and toxicity profile to advance from Phase I to Phase II in clinical trials, repurposing of this compound may represent an opportunity for rapid translation for clinical therapy of CRPC patients.

Introduction

Prostate cancer (PCa) remains the most commonly diagnosed cancer for U.S. males, and ranks second in cancer mortality with over 33,000 deaths expected this year [1]. Patients with localized PCa often undergo radiation or surgical therapy, which is curative for the majority of patients. However, a subset of patients will have recurrent disease, typically with metastases to the lymph nodes and bone. The standard of care for recurrent disease is hormonal androgen deprivation therapy (ADT) [2]; however, many patients progress during ADT, some quite rapidly. Recurrent disease that follows ADT treatment is termed castration-resistant prostate cancer (CRPC) [3,4], which is both aggressive and lethal. Approximately 10% to 20% of PCa patients progress to this state within 5 years [5]. Metastases are present in over 84% of CRPC patients, and the mean survival is around 14 months for metastatic CRPC patients [5]. Androgen receptor (AR) activity persists in most CRPC, with increased intratumoral androgen synthesis being a major mechanism driving this AR activity [6]. AR activity in CRPC can be suppressed by agents such as abiraterone, which further decrease androgen synthesis, or by AR antagonists such as enzalutamide. Enzalutamide (ENZ) [7] is a second generation AR antagonist that overcomes resistance to conventional anti-androgens by inhibiting nuclear localization and chromatin binding of AR [8,9], but patients still invariably progress. An increasingly recognized resistance mechanism to AR-directed therapy in prostate cancer involves epithelial plasticity, in which tumor cells demonstrate low to absent AR expression and often have neuroendocrine features [10–12]. Multiple mechanisms may contribute to persistent AR activity including alterations in the AR (AR gene amplification or activating mutations, expression of constitutively active AR splice variants, or AR posttranslational modifications), further increases in intratumoral androgen synthesis, and activation of multiple signaling pathways or epigenetic alterations that enhance tumor cell growth and may directly or indirectly enhance AR activity [6,13]. However, the contribution of any single mechanism to resistance is unclear, and multiple mechanisms may contribute to resistance in a single patient due to tumor heterogeneity. Thus, new targets and combination therapies are critically needed.

☆ FundingThis research was supported in part by the Dunwoody Golf Club Prostate Cancer Research Award, a philanthropic award provided by the Winship Invest$ Prostate Cancer Research Pilot Grant Program. Funding provided by the Evans County Cares foundation (JAP). Funding was also provided by NIH Grant No. U01 CA217875.

* Address all correspondence to: Carlos S. Moreno, Department of Pathology and Laboratory Medicine, Emory University, Atlanta, GA 30322, USA.
E-mail addresses: 410827310@qq.com, (Z. Li), qcsun@emory.edu, (C. Sun), sijia.tao@emory.edu, (S. Tao), aosunko@emory.edu, (A.O. Osunkoya), rsarnol@emory.edu, (R.S. Arnold), jpetros@emory.edu, (J.A. Petros), whzuxb@163.com, (X. Zu), cmoreno@emory.edu. (C.S. Moreno).

http://dx.doi.org/10.1016/j.tranon.2020.100751

Understanding the mechanisms underlying CRPC and subsequent progression to metastatic disease is critical to the development of more effective combination therapies. To gain insights into the response to ADT and emergence of CRPC, we performed RNAseq analysis of 20 patient-matched pre-ADT biopsies and 20 post-ADT radical prostatectomy (RP) prostate cancer samples and observed strong downregulation of AR targets and upregulation of genes involved in downstream of MAPK signaling, including FOS, FOSB, and JUN [14]. These data suggested that ADT may induce a compensatory increase in MAPK or JNK signaling in response to the decrease in androgen signaling.

Thus, we hypothesized that simultaneous and combined inhibition of both androgen and MAPK or JNK signaling may result in synergistic killing of prostate cancer cells. In this study we tested the effects of the MEK inhibitors PD0325901 and GSK1120212, ERK1/2 inhibitor GDC-0994, and the JNK inhibitor AS602801 alone and in combination with ENZ in androgen-sensitive cells and androgen-resistant prostate cancer cells. Here we show that ENZ combined with MEK or JNK inhibitors synergistically killed LNCaP and C4-2 cells, that the ENZ/ AS602801 combination prevents growth of tumor xenografts in immunocompromised mice, and that this combination results in a dramatic loss of AR mRNA and protein expression. These findings have potential implications for treatment of men with aggressive prostate cancer.

Materials and Methods

Materials

ENZ and GSK1120212, PD0325901, GDC-0994 were purchased from Selleckchem (Houston, TX) and were dissolved in DMSO to prepare 50 mM, 10 mM, 50 mM, and 1 mM stock solutions, respectively. AS602801 was purchased from Cayman Chemical (Ann Arbor, MI) and was dissolved in DMSO to prepare a 25 mM stock solution. AS602801 has previously been shown to be a highly specific JNK inhibitor [15]. SP600125 also inhibits JNK as a reversible ATP-competitive inhibitor with more than 20-fold selectivity over other kinases including Erk, p38 MAPKs, MKKs, and PKCs [16,17] and was a kind gift of Dr. Haian Fu (Emory University). All stock solutions were stored at −20°C for *in vitro* studies. For *in vivo* experiments, the ENZ stock solution was diluted in 20% Kolliphor RH40 (Sigma-Aldrich) to prepare 200 μl solutions for each injection. Antibodies were purchased from Cell Signaling Technology, Inc.: Phospho-SAPK/JNK (Cat #9251), SAPK/JNK (Cat #9252), Phospho-c-Jun (Cat #9261), C-Jun (Cat #9165), Phospho-Erk1/2 (Cat #9101), Erk1/2 (Cat #9102), PSA/KLK3 (Cat #5365), AR (Cat #3202), and GAPDH (Cat #2118).

Cell Culture

The prostate cell line LNCaP, C4-2, 22RV1, PC3 and DU145 were obtained from American Type Culture Collection. They were maintained in RPMI 1640 media supplemented with 10% FBS, 1% L-glutamine, and 1% penicillin-streptomycin. Cells were cultured in a 37°C incubator with humidified atmosphere of 5% CO2. All the cell lines were confirmed mycoplasma free using Mycoplasma PCR Detection Kit (abm Cat. No. G238). Cell lines were authenticated by IDEXX BioResearch and the Emory Integrated Genomics Core Facility.

Transfections and Transductions

Generation of luciferase expression in LNCaP cells: pLenti PGK V5-LUC Puro was a gift from Eric Campeau & Paul Kaufman (Addgene plasmid # 19360). The virus particles were generated by transfecting 293 T producer cells with pLenti PGK V5-LUC Puro expression vector and FuGENE® HD Transfection Reagent according to the manufacturer's guideline (Promega, Cat. No. E2311). Lentivirus was harvested from the supernatant 48 hours and 72 hours post transfection. LNCaP cells were infected with harvested lentiviral particles combined with polybrene at final concentration 8 μg/ml and incubated for 48 hours. The infected target cells were selected and cultivated in completed RPMI 1640 with 1 μg/ml puromycin. The efficiency of transduction was tested by luciferase assay.

Cell Viability and Cytotoxicity Assays

LNCaP and C4-2 cells were plated 10,000 cells/well in 96-well white plates and treated with ENZ (1.56, 3.125, 6.25, 12.5, 25, 50 μM); AS602801 (0.9375, 1.875, 3.75, 7.5, 15, 30 μM); GSK1120212 (1.56, 3.125, 6.25, 12.5, 25, 50 μM); PD-0325901 (3.125, 6.25, 12.5, 25, 50, 100 μM); GDC-0994 (0.0625, 0.125, 0.25, 0.5, 1, 2 μM) alone and combination for 48 hours using constant Ratio combination. Cell viability and cell death were assessed using RealTime Glo™ MT Cell Viability Assay and CellTox Green® Assays. Luminescence values and fluorescence were read using a Synergy HTX plate reader (BioTek Instruments, Inc.). Pooled results of biological triplicates with technical triplicates are shown after transforming the actual luminescence values into relative of control (DMSO 0.1%). Synergy between AS602801, GSK1120212, PD0325901, GDC-0094 and ENZ were evaluated according to the cell viability (% of control) by the Chou-Talalay combination index method. CompuSyn was used to calculate the combination index (CI) values using the constant Ratio Combination Design. Drug combinations that yielded CI values <1 were considered to be synergistic.

Cell Proliferation Assays

To evaluate proliferation, LNCaP cells were plated at 5000 cells/well in 96-well plates and treated with DMSO 0.1% (control); ENZ (12.5 μM); AS602801 (7.5 μM); GSK1120212 (12.5 μM); PD-0325901 (25 μM); GDC-0994 (1 μM) alone and combination. MTT assays were used to determine the number of cells at indicated concentrations by measuring the absorption at OD570 daily for 5 consecutive days. Each sample was assayed in triplicate in three independent experiments.

Cell Migration and Invasion Assays

Cell invasion and migration were evaluated using Boyden Chamber assays. LNCaP and C4-2 cells were seeded in the upper compartment of a 24-well Boyden chamber containing Matrigel-coated 8-μm pore membranes (Corning Cat # 353097) at 1×10^5 cells per well and treated with DMSO 0.1% (control); ENZ (12.5 μM); AS602801 (7.5 μM); GSK1120212 (12.5 μM); PD-0325901 (25 μM); or GDC-0994 (1 μM) alone and combination in 300 μl serum-free RPMI 1640 media and 500 μl of complete RPMI 1640 media (supplemented with 10% FBS, 1% penicillin-streptomycin, 1% L-glutamine) in the bottom chamber as a chemoattractant. After incubation for 24 hours at 37°C, non-invaded cells in the upper chamber were wiped away with a cotton swab and the filters then fixed and stained in 0.5% crystal violet for 10 minutes, then washed 3 times in ddH2O. ddH2O was aspirated and membranes allowed to dry for 2 hours in a cell culture biosafety cabinet. Membranes were then visualized under an upright confocal microscope using 40x magnification on a Nikon Eclipse Ti-S inverted microscope. For migration assays, cells were seeded at the same cell density and format in wells without Matrigel-coating. Representative images from 2 to 3 random fields were taken for each chamber. Cells were counted using Fiji open source analysis software (https://fiji.sc/). Each sample was assayed in triplicate in three independent experiments.

Protein Binding of AS602801 to Serum Proteins

Protein binding of AS602801 in RPMI 1640 cell culture media with 10% FBS was evaluated using the rapid equilibrium dialysis (RED) method as described in other publications [18,19]. The single-use plate RED device with dialysis membrane of molecular weight cut-off of approximately 8 K Da (ThermoFisher Scientific, Waltham, MA, USA) was used according to vendor's protocol. Aliquots of 300 μl of cell media with 10% FBS (containing 7.5 μM of AS602801 pre-incubated at 37°C for 30 minutes) and 550 μl of dialysis buffer (serum-free cell media) were added to sample

chambers and buffer chambers, respectively. The loaded plate was sealed and incubated at 37°C for 4 hours on an orbital shaker at 300 rpm. Upon completion of incubation, 50 μl aliquots were removed from each chamber. Then equal amount of serum-free cell media and media containing 10% FBS were added to sample and buffer respectively to generate matched matrix. All of the samples were then diluted with 400 μl of 100% acetonitrile containing internal standard and subjected to LC-MS/MS analysis. The percentage of free AS602801 was calculated by measuring its concentration in the buffer and sample chambers from peak area relative to internal standard. The concentration in the buffer chamber divided by concentration in sample chamber then multiplied by 100 is the unbound percentage. The final unbound value represents the mean of three replicates.

Western Blots

Cells were washed twice with 1X PBS and harvested with RIPA lysis buffer (Sigma Cat # R0278) containing protease inhibitors (Sigma Cat # P8340) and phosphatase inhibitors (Roche Cat # 4906845001). Whole cell lysates were centrifuged at 10,000 rpm for 10 minutes at 4°C. Supernatants were transferred to fresh tubes and protein concentration was quantified using the Pierce Bradford protein assay (Thermo Fisher Cat # 23225). Thirty μg of protein was analyzed on a 10% SDS-polyacrylamide gel by SDS-PAGE electrophoresis and transferred to a PVDF membrane (Biorad Cat #1620177). Membranes were blocked in 1X TBS buffer containing 5% BSA and 0.001% Tween for 1 hour at room temperature, and then incubated with primary antibody Phospho-SAPK/JNK (1:1000), SAPK/JNK (1:1000), Phospho-c-Jun (1:1000), C-Jun (1:1000), Phospho-Erk1/2 (1:1000), Erk1/2 (1:1000), PSA (1:3000), AR (1:1000), or GAPDH (1:5000) overnight at 4°C. Blots were washed with TBST three times for 5 minutes each and incubated with secondary antibodies (anti-rabbit IgG – Abcam # ab6721 1:10,000) for 1 hour at room temperature. Signals were visualized using SuperSignal West Pic PLUS chemiluminescence substrate (Pierce Cat #34580) according to the manufacturer's instructions (Thermo Fisher Scientific) and captured on film. Quantitative measurements of Western blot analysis were performed using Fiji and GraphPad software (Prism 7).

mRNA Analysis by QRT-PCR and Nanostring

Total RNAs were extracted from treated cells after 48 hours using TRizol reagent (Invitrogen). All RNA was converted to cDNA using iScript cDNA Synthesis Kit (Cat # 1708890). The cDNAs were subjected to real-time reverse transcription-PCR (RT-PCR) using SsoAdvanced Universal SYBR Green Supermix (Cat# 1725271) according to the manufacturer's instructions. Each reaction was normalized by co-amplification of beta actin. Triplicates of samples were performed with default settings on a Bio-Rad CFX-96 real-time cycler. Primers used for real-time PCR were: AR: Fwd 5′-GGAATTCCTGTGCATGAAA-3′; Rev. 5′-CGAAGTTCATCAAAGAATT-3′; Actin: Fwd 5′-AGA ACT GGC CCT TCT TGG AGG-3′; Rev. 5′-GTT TTT ATG TTC CTC TAT GGG-3′.

RNA samples were analyzed for integrity using the Nanostring Pan-Cancer Pathway Panel of 770 genes on an nCounter instrument at the Emory Integrated Genomics Core Facility. Normalized signal data was analyzed using the significance analysis of microarrays (samr) package [20] in R-Bioconductor using an FDR cutoff of $q < 0.05$. Hierarchical clustering was performed using Cluster [21] and Java Treeview [22] software.

Xenograft Experiments

After approval from the Institutional Animal Care and Use Committee, 32 male /CRL NU(NCr)-Foxn1 athymic nude mice (4- to 6-week-old) were purchased from Charles River Laboratories, Inc. Using a cold syringe and 27-gauge needle, $3x10^6$ LUC-LNCaP cells in a total volume of 0.2 ml serum-free medium containing 50% matrigel (BD Biosciences, Palo Alto, CA, USA) were injected subcutaneously into the neck under isofluorane anesthesia. Mice were monitored for approximately 4 weeks until palpable tumors grew to approximately 50 to 100 mm^3. Mice were randomized into four groups (with 5 to 6 tumors in each group) and injected daily follows: (i) vehicle control (10% DMSO, 20% Kolliphor RH40, i.p.), [23] ENZ (10 mg/kg, i.p), (iii) AS602801(10 mg/kg, i.p.), (iv) ENZ + AS602801 (10 mg/kg + 10 mg/kg, i.p). The 10 mg/kg doses used for ENZ [24] and for AS602801 [25] were the same as previously described. Tumor burden was assessed every 2 days by caliper measurement of two diameters of the tumor (LxW = mm2) and reported as tumor volume ((LxW2)/2 = mm3). Bioluminescence imaging to assess tumor size and viability was carried out at endpoint of treatment on an IVIS Spectrum Bioluminescence Imaging System (PerkinElmer) following intraperitoneal injection of 1.5 mg of d-luciferin (PerkinElmer). Measurements were performed when signal reached maximal plateau. Each group of mice was scanned separately in supine position, using high-exposure parameters. All applicable institutional and/or national guidelines for the care and use of animals were followed in this process.

Immunohistochemistry

Formalin-fixed paraffin-embedded tumor tissues from mouse xenografts were stained using antibodies to the androgen receptor (ThermoFisher Scientific Catalog # MA5-13426, 1:25 dilution) and to Ki67 (Abcam Catalog #ab16667, 1:300 dilution). Slides were stained on a DAKO autostainer at the Cancer Tissue and Pathology Core Shared Resource at the Winship Cancer Institute using standard protocols. Androgen receptor staining was quantified on a scale of 0 = no staining, 1 = weak staining, 2 = moderate staining, and 3 = strong staining. In addition, sections were scored on a scale of 0% positive nuclei, 1% to 25% positive, 26% to 50% positive, 51% to 75% positive, and 76% to 100% positive.

Statistical Analysis

Data analyses are expressed as the mean ± SD. Statistical significance where appropriate was evaluated using a two-tailed Student t test when comparing two groups, or by one-way analysis of variance (ANOVA) followed by Dunnett's posttest for multiple comparison. *, $P < .05$; **, $P < .01$; ***, $P < .001$; ****, $P < .0001$ were considered statistically significant; ns, not significant. Statistical analyses were performed using GraphPad Prism 7 software.

Results

Targeting AR and JNK/MEK Pathways Synergistically Decreases Viability of Prostate Cancer Cells and Inhibits Proliferation of Prostate Cancer Cells

The AR-positive human prostate cell line LNCaP was assessed for its response to ENZ and AS602801, GSK1120212, PD0325901, GDC-0994. All of these drugs significantly decreased viability of LNCaP cells in a concentration-dependent manner (Figure 1 and Supplementary Figure S1). Surprisingly, AS602801 was much more potent than any other single drug in decreasing cell viability. Moreover, the combination of ENZ with AS602801, GSK1120212, or PD0325901 significantly decreased viability of LNCaP cells (Figure 1*A* and Supplementary Figure S1). Similar results were observed in AR-positive, hormone-independent C4-2 cells (Figure 1*B*) and in castration-resistant 22Rv1 cells (Figure 1*C*). Moreover, AS602801 strongly reduced viability of castration-resistant DU145 and PC3 cells in a dose dependent manner (Figure 1*D*). Furthermore, we quantified the synergy between these combinations using CompuSyn software, which uses the Chou-Talalay algorithm to calculate combination index (CI) values with CI values < 1 considered to be synergistic [26,27]. The calculated CI values are depicted at ED50, ED75 and ED90 of each combination (Supplementary Figure S1). Synergy was observed between ENZ combined with AS602801, GSK112021, or PD0325901. Strong synergism ($0.1 < CI < 0.3$) between ENZ and GSK112021 was observed at ED90 (CI = 0.26) compared to AS602801 (CI = 0.63) or PD0325901 (CI = 0.64). To better assess drug effects, cell

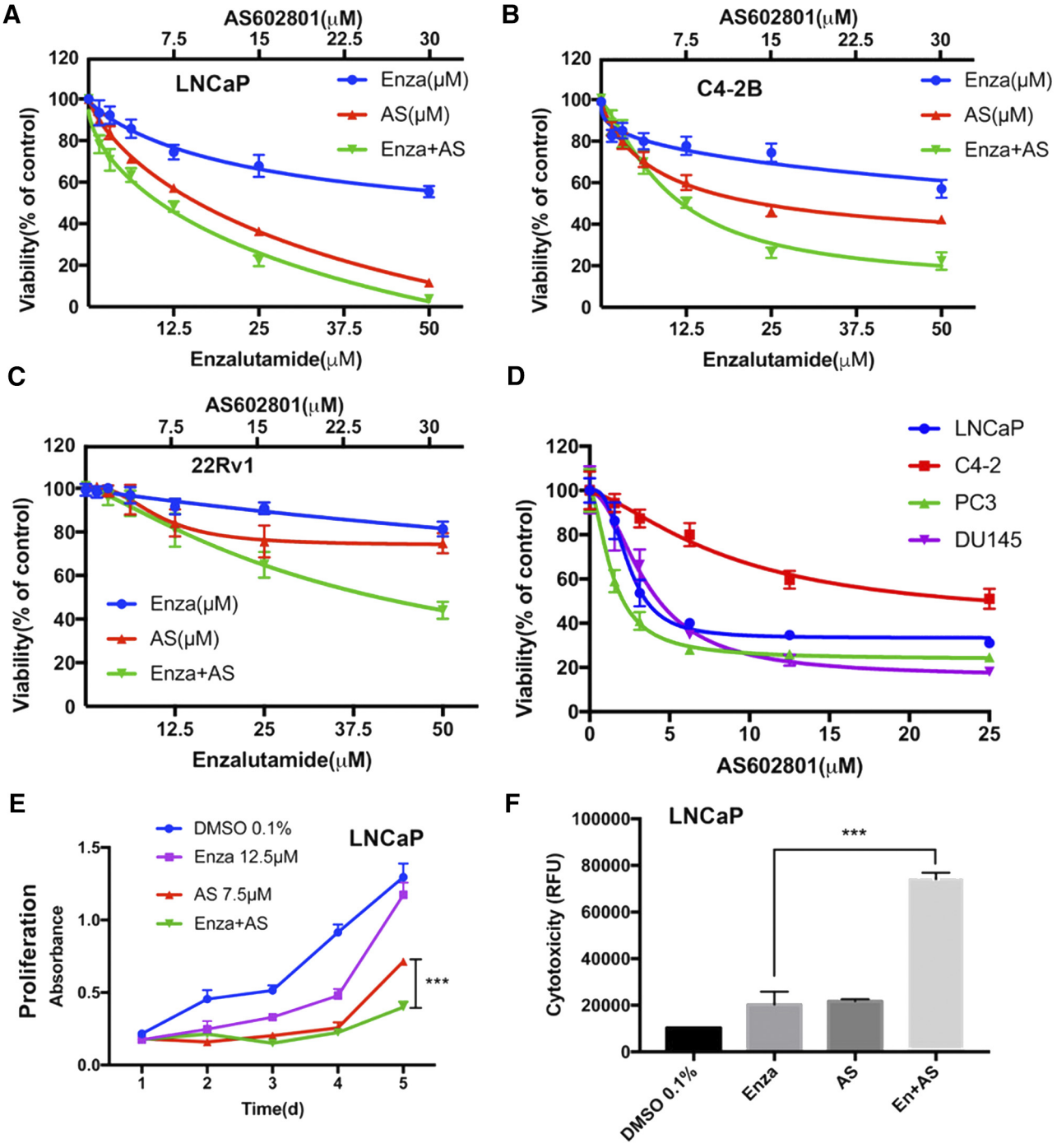

Figure 1. Effect of Enzalutamide and AS602801 on cell viability, proliferation, and cytotoxicity. LNCaP (A), C4-2 (B), or 22Rv1 (C) cells were plated 10,000 cells/well in 96-well plates and treated with ENZ, AS602801, or both and cell viability was assessed using RealTime Glo™ MT Cell Viability Assay. (D) Viability for LNCaP, C4-2, PC3, and DU145 cells over a range of concentrations of AS602801 is shown. (E) Proliferation of LNCaP cells was assayed by MTT at the indicated concentrations over a 5 day time course. (F) Cell death of LNCaP cells after 48 hr. incubation with ENZ (12.5 μM), AS602801 (7.5 μM), or both was measured using CellTox Green® assay, indicating strong synergy with the combination.

cytotoxicity assays were conducted by measuring plasma membrane leakage. ENZ and AS602801 had significant effects on cytotoxicity of LNCaP cells, whereas GSK112021, PD0325901 and GDC-0994 did not have significant effects. From these studies we determined the LD50 of AS602801 to be 7.5 μM, which was somewhat higher than expected, and raised concerns about off-target effects. We hypothesized that much of the drug could be bound up by FBS in the media or plastic in tissue culture plates. To test this hypothesis we performed a rapid equilibrium dialysis (RED) experiment as described [18,19] to determine the amount of free drug by LC-MS/MS and found that 98.7% was bound by serum proteins in cell culture media (see Methods), and that treatment of cells with 7.5 μM AS602801 results in an effective concentration of 97.5 nM, which is likely within a specific range given the potential for suboptimal cell permeability. In addition, the combination of ENZ with AS602801 significantly ($P = .0001$) reduced cell proliferation compared with single drug treatment (Figure 1*E*) and increased cytotoxicity (Figure 1*F*). Significant effects on proliferation and cytotoxicity were also observed for combination of ENZ with GSK1120212 and PD0325901 (Supplementary Figure S2). To determine if other JNK

inhibitors were similarly toxic to PCa cells, we tested the JNK inhibitor SP600125 [16,17] at a range of concentrations and found that LNCaP cells had an LD50 of 8.6 μM for SP600125 treatment (Supplementary Figure S3). Collectively, these data demonstrate that combined ENZ and AS602801 synergistically induce prostate cancer cell death and inhibit proliferation.

Targeting AR and JNK/MEK Pathways Inhibit Migration and Invasion of Prostate Cancer Cells

Transwell migration experiments were performed to further investigate whether combinations of ENZ with AS602801, GSK1120212, PD0325901, or GDC-0994 affected the ability of LNCaP cells to migrate and invade. We observed that AS602801 strongly inhibits LNCaP (Figure 2*A*) and castration-resistant C4-2 (Figure 2*B*) cell migration as well as invasion (Figure 2*C*) of LNCaP cells. Quantitative results indicated that the number of cells with the ability to migrate and invade was significantly reduced in the combination groups compared to the control groups except for the combination of ENZ and GDC-0994 in migration (Supplementary Figure S4). Additionally, ENZ alone can inhibit migration and invasion of LNCaP cells compared to control groups (Figure 2). Interestingly, the JNK inhibitor AS602801 alone inhibited migration and invasion of LNCaP cells more potently than any ENZ combinations with MEK or ERK inhibitors (Supplementary Figure S3). These assays were conducted after 24 hours of drug treatment, at which timepoint our proliferation assays (Figure 1*E*) indicate that the difference in cell number would be no more than 50%, and thus, the effects of AS602801 on migration and invasion cannot be due to reduced cell number alone. Surprisingly, we observed that GSK1120212, PD0325901, GDC-0994 also reduced of migration of C4-2 cells (Supplementary Figure S4), even though they had little effect on migration of LNCaP cells.

Combination Therapy with ENZ and AS602801 Blocks Prostate Cancer Growth in a LNCaP Xenograft Model

Our *in vitro* studies demonstrated that the combination of ENZ and AS602801 was the most effective in killing LNCaP cells and inhibiting migration and invasion. To test whether these effects were also the case in

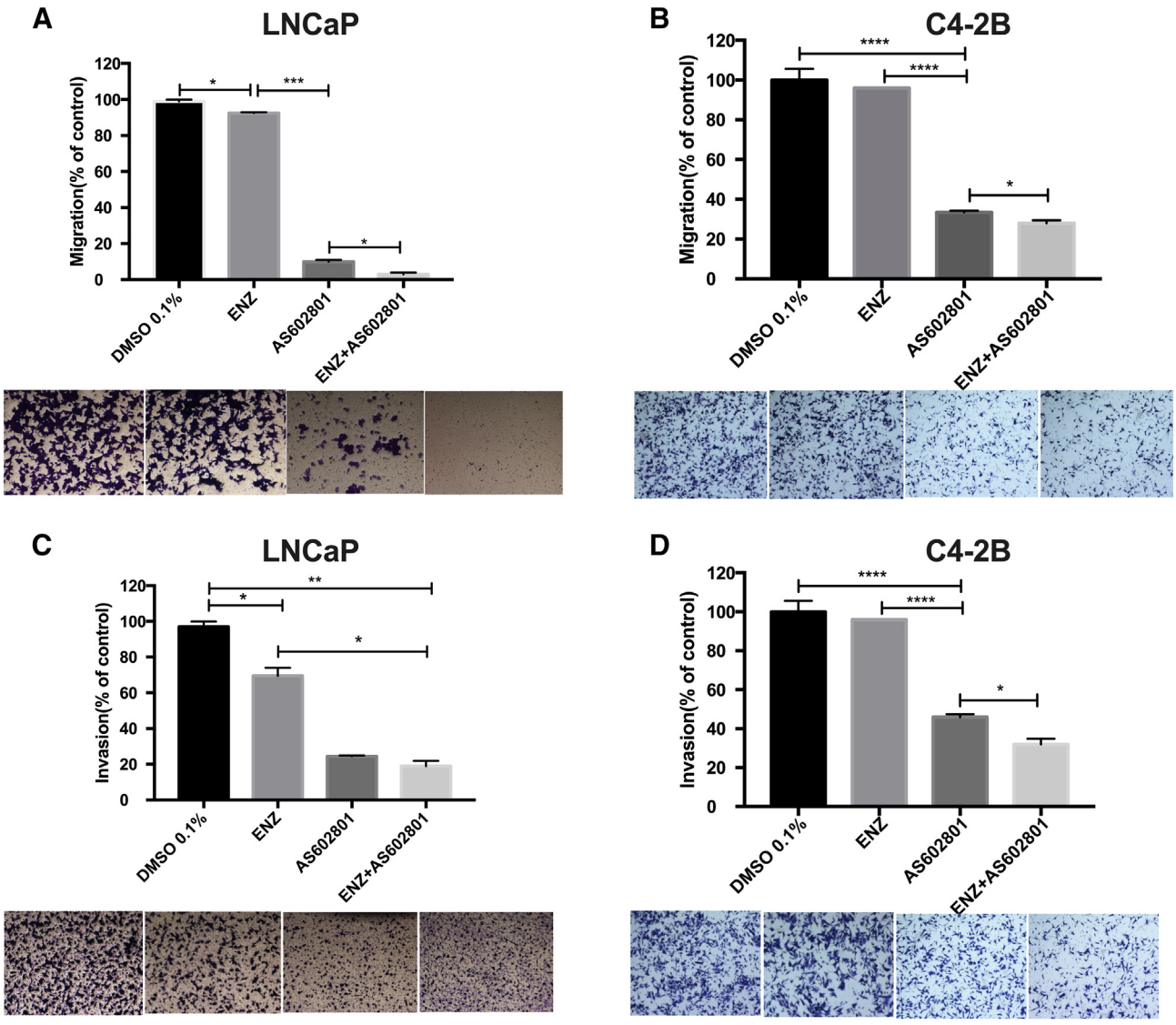

Figure 2. AS602801 synergizes with ENZ to inhibit LNCaP and C4-2B cell migration and invasion. (**A**) LNCaP cells were seeded in the upper chamber of a 24-well transwell at 1×10^5 cells per well treated with DMSO 0.1%(control); enzalutamide (12.5 μM); AS602801 (7.5 μM); or the combination for 24 hours. Migrating cells were imaged and counted using Fiji. (**B**) Same as in (A) with C4-2B cells. (**C**) LNCaP cells were seeded in the upper compartment of a 24-well invasion chamber at 1×10^5 cells per well treated as above. Invaded cells were imaged and counted using Fiji. (**D**) Same as in (C) with C4-2B cells. The data are shown as the mean ± SD of three experiments. $^*P < .05$, $^{**}P < .01$, $^{***}P < .001$.

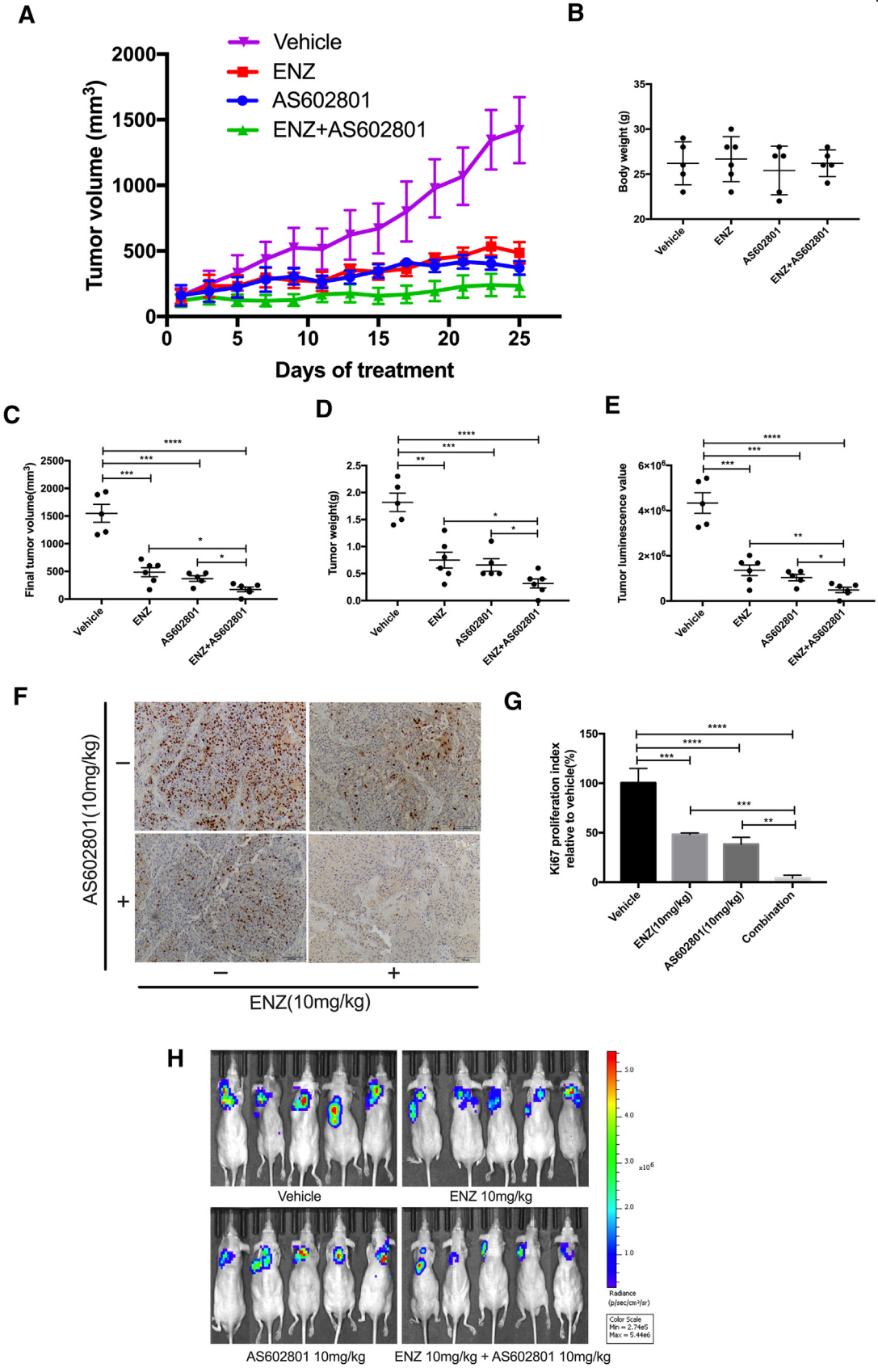

Figure 3. ENZ/AS602801 combination treatment in Luc-LNCaP xenografts. (**A**) Tumor growth of Luc-LNCaP xenografts treated with the indicated drugs for 25 days is presented. (**B**) Total body weight of mice is not affected by drug treatment. (**C**) Final tumor volume of the LNCaP xenograft tissues. (**D**) Final tumor weight of the LNCaP xenograft tissues. (**E**) Quantification of luciferase luminescence imaging before euthanasia of mice. (**F**) Immunohistochemistry of representative tumors stained for Ki67 to assess total proliferation. (**G**) Quantification of Ki67 IHC data. (**H**) Bioluminescence imaging of mice. Statistical analysis was performed with Student's t-test, $*P < .05$, $**P < .01$, $***P < .001$. $****P < .0001$.

inhibition of tumor growth *in vivo*, we generated subcutaneous Luciferase-LNCaP xenografts in immunodeficient male mice. Intact, non-castrated mice were used to enable engraftment of hormone-dependent LNCaP xenografts. Animals were administered ENZ and/or AS602801 as described in the Materials and Methods over the course of 25 days. As shown in Figure 3*A*, monotherapy with ENZ or AS602801 partially suppressed tumor growth, but the inhibitory effect was much stronger for combined ENZ plus AS602801. No significant side effects were observed for overall body weight (Figure 3*B*). Although both endpoints for tumor volume (Figure 3*C*) and mass (Figure 3*D*) were reduced with ENZ or AS602801 monotherapy, the effect was more significant with combinatory treatment (Figure 3, *C–E*). Immunohistochemistry staining for Ki-67 showed strongly reduced proliferation in combination treated tumors (Figure 3*F*). IHC staining for AR protein levels in xenografts demonstrated some downregulation of AR expression in AS602801 treated cells, but the variability in these data did not reach statistical significance (Supplementary Figure S5). Additionally, tumor size and viability were measured by Bioluminescence Imaging, which demonstrated consistent results and showed that there were no metastases present at the endpoints (Figure 3, *E* and *H*), which is not surprising because LNCaP subcutaneous xenografts generally do not metastasize. In short, these results indicated that the combination of ENZ and AS602801 most effectively inhibited prostate tumor growth *in vivo*. The JNK inhibitor AS602801 had sufficient safety and toxicity profile to advance from Phase I to Phase II in clinical trials for inflammatory endometriosis (NCT01630252), and thus repurposing of this compound may represent an opportunity for rapid translation of our findings.

AS602801 Dramatically Decreases AR Protein Levels in LNCaP Cells

To confirm the activity of ENZ on AR signaling, we analyzed expression of AR protein and its downstream target prostate specific antigen (PSA) by western blot. Surprisingly, the combination of ENZ and AS602801 or GSK1120212 dramatically decreased AR protein expression, as compared with ENZ alone ($P = .0027$, $P = .0468$) (Figure 4, *A* and *B*). The combination of ENZ and PD0325901 also decreased AR proteins levels compared with ENZ, although there was no statistical significance (Figure 4*C*). We did not observe any significant decrease of AR protein with combination ENZ and GDC-0994 although p-Erk was inhibited by GDC-0994 (Figure 4*D*). Moreover, treatment with AS602801 blocked JNK activation in response to anisomycin over 30 minutes (Figure 4*A*), and p-Erk was inhibited by GSK1120212 or PD0325901 alone or in combination with ENZ, as expected. Surprisingly, AS602801 was able to inhibit AR expression and activity more potently than ENZ as measured by decreases in AR and PSA protein (Figure 4*A*). Furthermore, the JNK inhibitor SP600125 also dramatically inhibited AR expression (Supplementary Figure S3*B*), demonstrating that the effects of AS602801 on AR expression are due to JNK inhibition. Taken together, these results suggest that AS602801 can negatively regulate AR protein levels.

AS602801 Treatment Increases c-Jun Phosphorylation, Activates JNK Signaling, and Blocks AR Expression at the mRNA Level

Our results indicate that treatment of LNCaP cells and C4-2 cells with the JNK inhibitor AS602801 results in a dramatic decrease in AR protein levels (Figure 4, *A* and *G*), but the mechanisms are not well understood. To determine whether AR transcript levels were reduced, we performed quantitative real-time PCR (QPCR) following AS602801 treatment of LNCaP cells and observed that AS602801 potently inhibited AR mRNA expression (Figure 4*F*). Interestingly, we also observed that although treatment of LNCaP cells with ENZ reduced AR protein expression (Figure 4*A*), AR mRNA levels were dramatically increased by ENZ treatment (Figure 4*F*), possibly due to endogenous negative feedback mechanisms. The western blots also showed that AS602801 decreased AR protein expression with time-dependent manner (Figure 4*E*). It has been reported that there are direct protein-protein interactions between AR and c-Jun proteins that might affect AR function [28]. To explore whether AS602801 also affects the expression of AR and AR-V7 mRNA in C4-2 cells, we performed QPCR following AS602801 treatment of C4-2 cells and observed that AS602801 potently inhibited both AR and AR-V7 mRNA expression (Figure 4*H*). This is consistent with previous studies [29] showing that JNK activation can repress transcription of the AR gene. In short, these results suggested that induction of c-Jun activity by AS602801 might play an important role in down-regulation of AR expression and activity.

Interestingly, incubation of unstimulated LNCaP cells with AS602801 over 24 hours actually increases c-Jun phosphorylation and JNK activation (Figure 4*E*), suggesting that AS602801 may actually increase rather than decrease activity of c-Jun which could in turn inhibit transcription of the AR gene. This suggests that there is a delayed response to the drug that requires at least 24 hours to activate JNK following AS602801 treatment. To help elucidate the mechanisms of cell death and the effects of AS602801 on JNK activity, we performed focused gene expression analysis using the Nanostring Pan-Cancer pathway panel that interrogates 770 genes from 13 cancer-associated canonical pathways. We identified 230 genes that were significantly differentially expressed between AS602801-treated and control cells (FDR < 0.05) (Supplementary Table S1), and 327 genes differentially expressed between control cells and cells treated with the combination of AS602801 and ENZ (Supplementary Table S2). Gene ontology analysis of the 230 significant genes affected by AS602801-treatment demonstrated that there was a highly significant enrichment of genes associated with the cell cycle that were altered (FDR = 8.5e-8), even after correcting for the fact that there were only 770 genes on the panel and they were all associated with cancer related pathways. To further analyze how the AS602801-treatment affected AR signaling, JNK signaling, and the cell cycle, we extracted 104 significant genes annotated for these pathways and performed hierarchical clustering analysis (Figure 5*A*). Genes associated with cell cycle arrest were strongly upregulated, while genes associated with cell cycle progression were strongly downregulated upon treatment with AS602801 or combined AS602801 and ENZ. Furthermore, the nanostring data confirmed the effectiveness of ENZ in repression of AR target gene TMPRSS2 and the repression of AR mRNA by AS602801. JNK pathway activation is essential for TNF-induced apoptosis [30] and sensitizes prostate cancer cells to FAS-induced apoptosis [31]. Moreover, JNK activity induces expression of GADD45 genes [32]. Nanostring Pan-Cancer Pathway Panel analysis of cells treated with AS602801 (Figure 5*B*) shows that AS602801 strongly upregulates GADD45A/B/G, TNF, and FAS expression (15.3-fold, 19.0-fold, 3.3-fold, 4.3-fold and 3.7-fold, respectively), suggesting activation of JNK-signaling and JNK-dependent apoptosis. Treatment of LNCaP and C4-2 cells with AS602801 induced PARP cleavage and Caspase-3 cleavage, consistent with induction of apoptosis (Figure 5, *C* and *D*). Furthermore, combined AS602801/ENZ treatment induced MAPK10 (JNK3) 2.6-fold and repressed TMPRSS2 (-5.1 fold), while AS602801 alone did not induce JNK3 or repress TMPRSS2. These data suggest that sustained AS602801-treatment combined with ENZ can induce JNK3 expression, activate JNK signaling, repress AR signaling, and induce apoptosis.

Discussion

Many strategies used to kill cancer cells induce stress and survival responses that promote the emergence of treatment resistance, which is the underlying basis for most cancer deaths. In prostate cancer, androgen deprivation therapy induces apoptosis and clinical responses in most patients but also triggers progression to CRPC. Similarly, newer AR pathway inhibitors such as abiraterone and ENZ prolong patient survival but resistance frequently develops in many initial responders [33,34]. Disease progression often correlates with rising PSA levels, indicating continued AR signaling and highlighting the need for additional therapies that target the molecular basis of treatment-resistant CRPC. Defining interactions between the AR and redundant survival pathways will build new combinatorial strategies that control progression and improve outcomes.

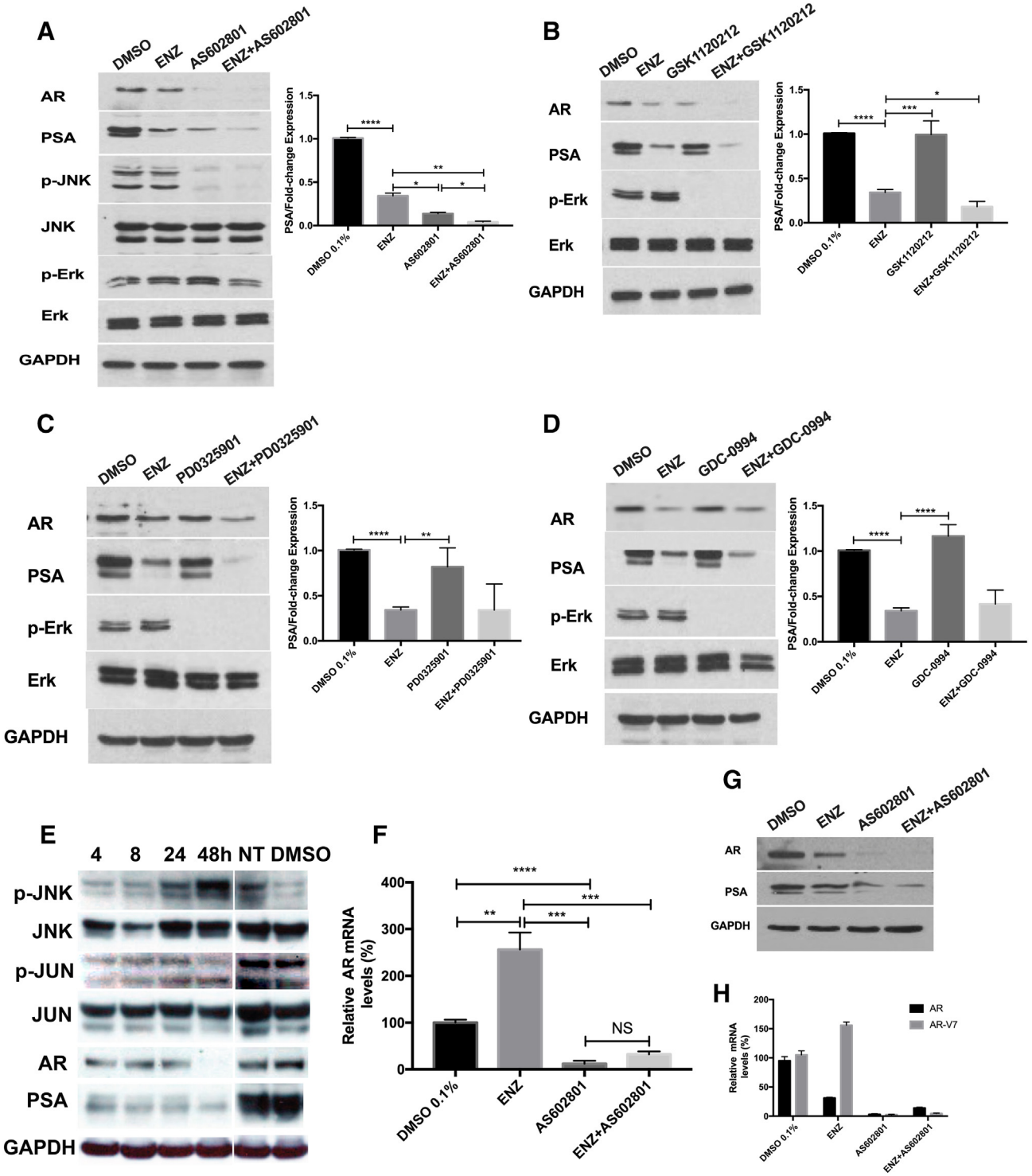

Figure 4. Effect of Enzalutamide and/or AS602801, GSK1120212, PD-0325901, GDC-0994 on pathway protein and mRNA expression. (A-D) LNCaP cells (1×10^6 cells) were seeded in 6-well plates and incubated for 24 h to allow for adherence. Cells were treated with DMSO 0.1% (control); enzalutamide (12.5 μM); AS602801 (7.5 μM); GSK1120212 (12.5 μM); PD-0325901(25 μM); GDC-0994 (1 μM) alone and combination 48 h for PSA and AR detection. For p-Erk detection, LNCaP cells were pretreated with 5 μg/ml EGF for 1 h after 24 h starvation, then treated with indicated concentration for 1 h. For p-JNK detection, LNCaP cells were treated with indicated concentration for 2 hours, then stimulated with 25 μg/ml Anisomycin for 30mins. Western blot analysis was conducted for AR, PSA, p-ERK(Thr202/Tyr204)/ERK, p-JNK/JNK. GAPDH was used as loading control. (E) LNCaP cells were treated with AS602801 (7.5 μM) for various time points. AR/PSA, JNK, p-JNK, and p-c-Jun/c-Jun were analyzed by Western blot analysis; GAPDH was using as a loading control. NT indicates untreated LNCaP cells, and DMSO indicates LNCaP cells treated with vehicle for 48 hours. The expression level of PSA was quantified with Fiji. (F) LNCaP cells were treated with indicated concentrations for 48 h for RNA extraction and analyzed by QPCR. AR mRNA levels were normalized by co-amplification of beta-actin mRNA and are shown as relative fold change. (G) C4-2 cells were treated with DMSO 0.1% and enzalutamide (12.5 μM); AS602801 (7.5 μM) and combination. AR and PSA were analyzed by Western blot analysis; GAPDH was using as a loading control. (H) C4-2 cells were treated with indicated concentrations for 48 h for RNA extraction and analyzed by QPCR. AR and AR-V7 mRNA levels were normalized by co-amplification of beta-actin mRNA and are shown as relative fold change. All the experiments were repeated three times, and the data are presented as the mean ± SD. $^*P < .1$, $^{**}P < .01$, $^{***}P < .001$, $^{****}P < .0001$.

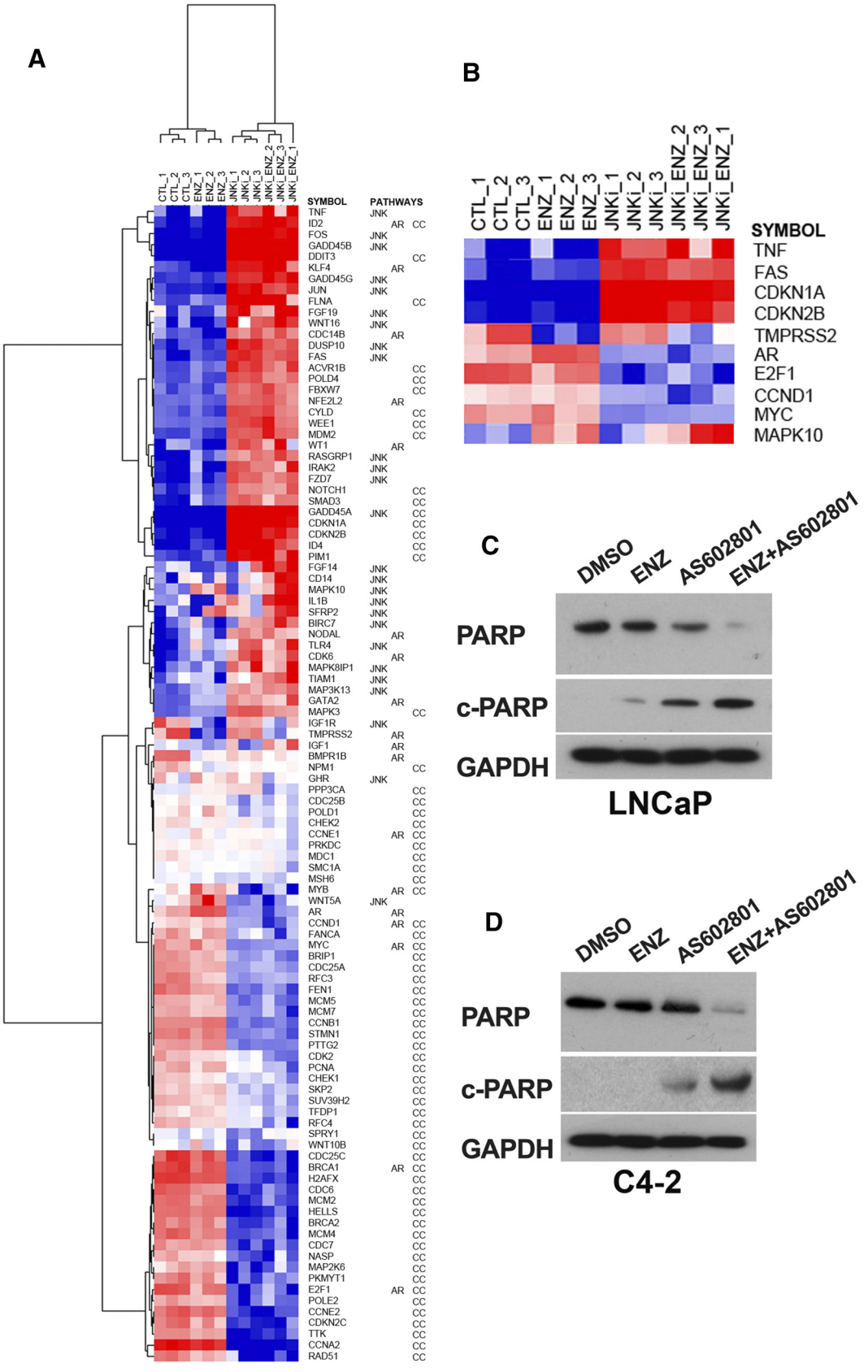

Figure 5. Nanostring analysis of AS602801 effects on LNCaP cells (A) Hierarchical clustering of 104 genes from nanostring mRNA signal data. LNCaP cells were treated with DMSO control, ENZ, AS602801, or combined AS602801/ENZ for 48 h and RNA harvested. One hundred four genes annotated for JNK, AR, or cell cycle (CC) pathways that were significantly different between AS602801-treated cells and controls were included in the cluster analysis. Gene symbols and the pathways for which each gene is annotated are indicated to the right. Red indicates increased mRNA and blue indicated decreased mRNA levels. (B) Subset of affected genes from hierarchical clustering. (C) Western blot for PARP in LNCaP cells indicates induction of apoptosis in AS602801-treated cells. (D) Similar blot for PARP in AS602801-treated C4-2 cells.

c-Jun N-terminal protein kinase (JNK) is a subfamily of the mitogen activated protein kinase (MAPK) superfamily [35,36]. The Stress Activated Kinase/JNK pathway mediates cellular responses to stresses such as UV radiation, inflammatory cytokines, and reactive oxygen species, and results in phosphorylation of c-Jun by JNK kinases, activation of p53, ATF3, SMAD4, c-Myc [37–39], ultimately inducting apoptosis or autophagy [36,39,40]. Several JNK inhibitor (JNKi) compounds have been developed, such as the competitive ATP inhibitor AS602801 [15], which is more specific than SP600125, which also inhibits p38 MAPK [41]. In prostate cancers, AR has been shown to inhibit JNK by inducing p21 and interfering with TNF/NFκB induced apoptosis [42]. AR can also inhibit JNK-mediated apoptosis in response to thapsigargin, the phorbol ester 12-O-tetradecanoyl-13-phorbol-acetate (TPA), or UV irradiation [43]. Phorbol 12-myristate 13-acetate (PMA) induces cellular apoptosis in LNCaP and C4-2B prostate cancer cells, and this apoptotic effect is mediated by JNK activation of p53 signaling [44]. However, mice with homozygous deletions of JNK1, JNK2, and PTEN in the prostate epithelium developed aggressive prostate cancers that metastasize and have increased stem-like phenotypes that are more resistant to androgen withdrawal [45], arguing that JNK inhibition would promote, rather than hinder aggressive disease. Thus, there are conflicting studies that suggest that inhibition of JNK could be undesirable by blocking apoptosis, or beneficial by inhibiting cellular proliferation, invasion, and metastasis.

In this study, we definitively demonstrate that the combination of the JNKi AS602801 with ENZ is highly synergistic for inducing cell death, blocking invasion, and inhibiting tumor growth of LNCaP prostate cancer cells *in vivo*. While treatment with AS602801 blocks JNK activation in response to anisomycin over 30 minutes (Figure 4*A*), incubation of unstimulated LNCaP cells with JNKi over 48 hours actually increases JNK phosphorylation and activity (Figure 4*E*). Furthermore, nanostring analysis of mRNA responses to AS602801 treatment indicate that this compound is activating JNK signaling after 48 hours and this may be due to induction of JNK3 expression. Thus, it is likely that the synergistic killing effects of AS602801 are due to JNK activation rather than JNK inhibition. We speculate that AS602801 may be metabolized over time and that by 48 hours, total JNK activity is increased rather than decreased due to compensatory negative feedback pathways that result in induction of JNK3. Moreover, AS602801 treatment clearly results in a profound loss of AR expression both in protein and mRNA levels, and it also downregulates the AR-V7 mRNA levels, which may partially explain the synergistic effects we observed, but the mechanism behind this phenomenon is not well understood. It is clear that this is due to on-target JNK inhibition, since SP600125 has similar effects, albeit with different pharmacokinetics. More research will be necessary to uncover these mechanisms in the future. Nevertheless, our data show that AS602801 has great potential as an effective drug candidate either as a monotherapy or, more likely, in combination with ENZ for treatment of advanced metastatic prostate cancer. This study demonstrates that combination therapies using AS602801 with ENZ may represent a potential strategy for new therapeutic approaches for patients with aggressive prostate cancer.

In summary, here we have shown that combinations of AS602801 with the androgen receptor inhibitor enzalutamide synergistically kill prostate cancer cells, inhibit proliferation, migration, and invasion, and prevent tumor growth in mouse xenografts. These findings immediately suggest the potential for combination drug clinical trials by repurposing the AS602801 drug together with enzalutamide for patients with aggressive prostate cancer.

Supplementary data to this article can be found online at https://doi.org/10.1016/j.tranon.2020.100751.

Author Contributions

ZL performed experiments, analyzed data, and wrote the original draft of the manuscript. CS performed experiments. ST performed experiments. AOO analyzed data and edited the manuscript. RA supervised experiments and edited the manuscript. JAP supervised experiments, provided funding, and edited the manuscript. XBZ provided funding and edited the manuscript. CSM supervised, conceptualized, administered, provided funding, wrote portions of the manuscript, and edited the manuscript.

Acknowledgments

The authors would like to thank Drs. Daniel Kalman, Raymond Schinazi, Selwyn Hurwitz, and James Kohler of Emory University for helpful discussions. We also thank Hongjing Zang for technical assistance. Research reported in this publication was supported in part by the Emory Integrated Genomics Core (EIGC) Shared Resource and the Cancer Tissue and Pathology Core Shared Resource of Winship Cancer Institute of Emory University and NIH/NCI under award number P30CA138292. This research was funded in part by NCI U01 CA168449 and in part by the Roswell Country Club Prostate Cancer Research Award, a philanthropic award provided by the Winship Cancer Institute of Emory University through the Winship Invest$ Prostate Pilot Grant Program. The content is solely the responsibility of the authors and does not necessarily represent the official views of the National Institutes of Health.

Declaration of Competing Interest

The authors declare no conflict of interest.

References

[1] ACS, Cancer Facts and Figures 2020, American Cancer Society, 2020.
[2] H. Beltran, T.M. Beer, M.A. Carducci, J. de Bono, M. Gleave, M. Hussain, W.K. Kelly, F. Saad, C. Sternberg, S.T. Tagawa, I.F. Tannock, New therapies for castration-resistant prostate cancer: efficacy and safety, Eur Urol 60 (2011) 279–290.
[3] Q. Wang, W. Li, Y. Zhang, X. Yuan, K. Xu, J. Yu, Z. Chen, R. Beroukhim, H. Wang, M. Lupien, T. Wu, M.M. Regan, C.A. Meyer, J.S. Carroll, A.K. Manrai, O.A. Janne, S.P. Balk, R. Mehra, B. Han, A.M. Chinnaiyan, M.A. Rubin, L. True, M. Fiorentino, C. Fiore, M. Loda, P.W. Kantoff, X.S. Liu, M. Brown, Androgen receptor regulates a distinct transcription program in androgen-independent prostate cancer, Cell 138 (2009) 245–256.
[4] F. Lian, N.V. Sharma, J.D. Moran, C.S. Moreno, The biology of castration-resistant prostate cancer, Curr Probl Cancer 39 (2015) 17–28.
[5] M. Kirby, C. Hirst, E.D. Crawford, Characterising the castration-resistant prostate cancer population: a systematic review, Int J Clin Pract 65 (2011) 1180–1192.
[6] I. Coutinho, T.K. Day, W.D. Tilley, L.A. Selth, Androgen receptor signaling in castration-resistant prostate cancer: a lesson in persistence, Endocr Relat Cancer 23 (2016) T179–t197.
[7] N. Agarwal, G. Di Lorenzo, G. Sonpavde, J. Bellmunt, New agents for prostate cancer, Ann Oncol 25 (2014) 1700–1709.
[8] C.S. Higano, T.M. Beer, M.E. Taplin, E. Efstathiou, M. Hirmand, D. Forer, H.I. Scher, Long-term safety and antitumor activity in the phase 1-2 study of enzalutamide in pre- and post-docetaxel castration-resistant prostate cancer, Eur Urol 68 (2015) 795–801.
[9] C. Tran, S. Ouk, N.J. Clegg, Y. Chen, P.A. Watson, V. Arora, J. Wongvipat, P.M. Smith-Jones, D. Yoo, A. Kwon, T. Wasielewska, D. Welsbie, C.D. Chen, C.S. Higano, T.M. Beer, D.T. Hung, H.I. Scher, M.E. Jung, C.L. Sawyers, Development of a second-generation antiandrogen for treatment of advanced prostate cancer, Science 324 (2009) 787–790.
[10] M.A. Nieto, Epithelial plasticity: a common theme in embryonic and cancer cells 342 (2013) 1234850.
[11] H. Beltran, D. Prandi, J.M. Mosquera, M. Benelli, L. Puca, J. Cyrta, C. Marotz, E. Giannopoulou, B.V. Chakravarthi, S. Varambally, S.A. Tomlins, D.M. Nanus, S.T. Tagawa, E.M. Van Allen, O. Elemento, A. Sboner, L.A. Garraway, M.A. Rubin, F. Demichelis, Divergent clonal evolution of castration-resistant neuroendocrine prostate cancer, Nat Med 22 (2016) 298–305.
[12] E.G. Bluemn, I.M. Coleman, J.M. Lucas, R.T. Coleman, S. Hernandez-Lopez, R. Tharakan, D. Bianchi-Frias, R.F. Dumpit, A. Kaipainen, A.N. Corella, Y.C. Yang, M.D. Nyquist, E. Mostaghel, A.C. Hsieh, X. Zhang, E. Corey, L.G. Brown, H.M. Nguyen, K. Pienta, M. Ittmann, M. Schweizer, L.D. True, D. Wise, P.S. Rennie, R.L. Vessella, C. Morrissey, P.S. Nelson, Androgen receptor pathway-independent prostate cancer is sustained through FGF signaling, Cancer Cell 32 (2017) 474–489e476.
[13] T. Karantanos, P.G. Corn, T.C. Thompson, Prostate cancer progression after androgen deprivation therapy: mechanisms of castrate resistance and novel therapeutic approaches, Oncogene 32 (2013) 5501–5511.
[14] N.V. Sharma, K.L. Pellegrini, V. Ouellet, F.O. Giuste, S. Ramalingam, K. Watanabe, E. Adam-Granger, L. Fossouo, S. You, M.R. Freeman, P. Vertino, K. Conneely, A.O. Osunkoya, D. Trudel, A.M. Mes-Masson, J.A. Petros, F. Saad, C.S. Moreno, Identification of the Transcription Factor Relationships Associated with Androgen Deprivation Therapy Response and Metastatic Progression in Prostate Cancer, Cancers (Basel), 10, 2018.
[15] S. Halazy, Designing heterocyclic selective kinase inhibitors: from concept to new drug candidates, ARKIVOC, vii (2006) 496–508.
[16] Y.S. Heo, S.K. Kim, C.I. Seo, Y.K. Kim, B.J. Sung, H.S. Lee, J.I. Lee, S.Y. Park, J.H. Kim, K.Y. Hwang, Y.L. Hyun, Y.H. Jeon, S. Ro, J.M. Cho, T.G. Lee, C.H. Yang, Structural basis

for the selective inhibition of JNK1 by the scaffolding protein JIP1 and SP600125, EMBO J 23 (2004) 2185–2195.
[17] B.L. Bennett, D.T. Sasaki, B.W. Murray, E.C. O'Leary, S.T. Sakata, W. Xu, J.C. Leisten, A. Motiwala, S. Pierce, Y. Satoh, S.S. Bhagwat, A.M. Manning, D.W. Anderson, SP600125, an anthrapyrazolone inhibitor of Jun N-terminal kinase, Proc Natl Acad Sci U S A 98 (2001) 13681–13686.
[18] K.C. Ferguson, Y.S. Luo, I. Rusyn, W.A. Chiu, Comparative analysis of rapid equilibrium dialysis (RED) and solid phase micro-extraction (SPME) methods for in vitro-in vivo extrapolation of environmental chemicals, Toxicol In Vitro 60 (2019) 245–251.
[19] S. Garcia-Martinez, E. Rico, E. Casal, A. Grisalena, E. Alcaraz, N. King, N. Leal, I. Navarro, M.A. Campanero, Bionalytical validation study for the determination of unbound ambrisentan in human plasma using rapid equilibrium dialysis followed by ultra performance liquid chromatography coupled to mass spectrometry, J Pharm Biomed Anal 150 (2018) 427–435.
[20] V.G. Tusher, R. Tibshirani, G. Chu, Significance analysis of microarrays applied to the ionizing radiation response, Proc Natl Acad Sci U S A 98 (2001) 5116–5121.
[21] M.B. Eisen, P.T. Spellman, P.O. Brown, D. Botstein, Cluster analysis and display of genome-wide expression patterns, Proc Natl Acad Sci U S A 95 (1998) 14863–14868.
[22] A.J. Saldanha, Java Treeview–extensible visualization of microarray data, Bioinformatics 20 (2004) 3246–3248.
[23] K. Saito, Y. Fujii, Antitumor activity and safety of enzalutamide after abiraterone acetate: seeking the optimal treatment sequence for castration-resistant prostate cancer patients, Eur Urol 74 (2018) 46–47.
[24] J. Wu, S. Moverare-Skrtic, A.E. Borjesson, M.K. Lagerquist, K. Sjogren, S.H. Windahl, A. Koskela, L. Grahnemo, U. Islander, A.S. Wilhelmson, A. Tivesten, J. Tuukkanen, C. Ohlsson, Enzalutamide reduces the bone mass in the axial but not the appendicular skeleton in male mice, Endocrinology 157 (2016) 969–977.
[25] S.S. Palmer, M. Altan, D. Denis, E.G. Tos, J.P. Gotteland, K.G. Osteen, K.L. Bruner-Tran, S.G. Nataraja, Bentamapimod (JNK Inhibitor AS602801) induces regression of endometriotic lesions in animal models, Reprod Sci 23 (2016) 11–23.
[26] T.C. Chou, The mass-action law based algorithm for cost-effective approach for cancer drug discovery and development, Am J Cancer Res 1 (2011) 925–954.
[27] T.C. Chou, Drug combination studies and their synergy quantification using the Chou-Talalay method, Cancer Res 70 (2010) 440–446.
[28] N. Sato, M.D. Sadar, N. Bruchovsky, F. Saatcioglu, P.S. Rennie, S. Sato, P.H. Lange, M.E. Gleave, Androgenic induction of prostate-specific antigen gene is repressed by protein-protein interaction between the androgen receptor and AP-1/c-Jun in the human prostate cancer cell line LNCaP, J Biol Chem 272 (1997) 17485–17494.
[29] S.V. Singh, S. Choi, Y. Zeng, E.R. Hahm, D. Xiao, Guggulsterone-induced apoptosis in human prostate cancer cells is caused by reactive oxygen intermediate dependent activation of c-Jun NH2-terminal kinase, Cancer Res 67 (2007) 7439–7449.
[30] Y. Deng, X. Ren, L. Yang, Y. Lin, X. Wu, A JNK-dependent pathway is required for TNFalpha-induced apoptosis, Cell 115 (2003) 61–70.
[31] A.P. Costa-Pereira, S.L. McKenna, T.G. Cotter, Activation of SAPK/JNK by camptothecin sensitizes androgen-independent prostate cancer cells to Fas-induced apoptosis, Br J Cancer 82 (2000) 1827–1834.
[32] Y. Ju, T. Xu, H. Zhang, A. Yu, FOXO1-dependent DNA damage repair is regulated by JNK in lung cancer cells, Int J Oncol 44 (2014) 1284–1292.
[33] W.P. Harris, E.A. Mostaghel, P.S. Nelson, B. Montgomery, Androgen deprivation therapy: progress in understanding mechanisms of resistance and optimizing androgen depletion, Nat Clin Pract Urol 6 (2009) 76–85.
[34] H.I. Scher, T.M. Beer, C.S. Higano, A. Anand, M.E. Taplin, E. Efstathiou, D. Rathkopf, J. Shelkey, E.Y. Yu, J. Alumkal, D. Hung, M. Hirmand, L. Seely, M.J. Morris, D.C. Danila, J. Humm, S. Larson, M. Fleisher, C.L. Sawyers, Antitumour activity of MDV3100 in castration-resistant prostate cancer: a phase 1–2 study, Lancet (London, England) 375 (2010) 1437–1446.
[35] R.J. Davis, Signal transduction by the JNK group of MAP kinases, Cell 103 (2000) 239–252.
[36] C.R. Weston, R.J. Davis, The JNK signal transduction pathway, Curr Opin Cell Biol 19 (2007) 142–149.
[37] M. Das, F. Jiang, H.K. Sluss, C. Zhang, K.M. Shokat, R.A. Flavell, R.J. Davis, Suppression of p53-dependent senescence by the JNK signal transduction pathway, Proc Natl Acad Sci U S A 104 (2007) 15759–15764.
[38] M. Hibi, A. Lin, T. Smeal, A. Minden, M. Karin, Identification of an oncoprotein- and UV-responsive protein kinase that binds and potentiates the c-Jun activation domain, Genes Dev 7 (1993) 2135–2148.
[39] E.F. Wagner, A.R. Nebreda, Signal integration by JNK and p38 MAPK pathways in cancer development, Nat Rev Cancer 9 (2009) 537–549.
[40] K. Sabapathy, Role of the JNK pathway in human diseases, Prog Mol Biol Transl Sci 106 (2012) 145–169.
[41] M. Okada, K. Kuramoto, H. Takeda, H. Watarai, H. Sakaki, S. Seino, M. Seino, S. Suzuki, C. Kitanaka, The novel JNK inhibitor AS602801 inhibits cancer stem cells in vitro and in vivo, Oncotarget 7 (2016) 27021–27032.
[42] F. Tang, J. Kokontis, Y. Lin, S. Liao, A. Lin, J. Xiang, Androgen via p21 inhibits tumor necrosis factor alpha-induced JNK activation and apoptosis, J Biol Chem 284 (2009) 32353–32358.
[43] P.I. Lorenzo, F. Saatcioglu, Inhibition of apoptosis in prostate cancer cells by androgens is mediated through downregulation of c-Jun N-terminal kinase activation, Neoplasia 10 (2008) 418–428.
[44] M. Itsumi, M. Shiota, A. Yokomizo, A. Takeuchi, E. Kashiwagi, T. Dejima, J. Inokuchi, K. Tatsugami, T. Uchiumi, S. Naito, PMA induces androgen receptor downregulation and cellular apoptosis in prostate cancer cells, J Mol Endocrinol 53 (2014) 31–41.
[45] A. Hubner, D.J. Mulholland, C.L. Standen, M. Karasarides, J. Cavanagh-Kyros, T. Barrett, H. Chi, D.L. Greiner, C. Tournier, C.L. Sawyers, R.A. Flavell, H. Wu, R.J. Davis, JNK and PTEN cooperatively control the development of invasive adenocarcinoma of the prostate, Proc Natl Acad Sci U S A 109 (2012) 12046–12051.